Quantitative Structure–Permeation Relationships for Solute Transport across Silicone Membranes

Sandrine Geinoz,[1] Sebastien Rey,[1] Gilles Boss,[1] Annette L. Bunge,[2] Richard H. Guy,[3] Pierre-Alain Carrupt,[1] Marianne Reist,[1] and Bernard Testa[1,4]

Received April 15, 2002; accepted July 30, 2002

Purpose. The purpose of this work was to assess the molecular properties that influence solute permeation across silicone membranes and to compare the results with transport across human skin.

Methods. The permeability coefficients (log K_p) of a series of model solutes across silicone membranes were determined from the analysis of simple transport experiments using a pseudosteady-state mathematical model of the diffusion process. Subsequently, structure–permeation relationships were constructed and examined, focusing in particular on the difference between solute octanol/water and 1,2-dichloroethane/water partition coefficients ($\Delta\log P_{oct\text{-}dce}$), which reported upon H-bond donor activity, and the computationally derived molecular hydrogen-bonding potential.

Results. The hydrogen-bond donor acidity and the lipophilicity of the compounds examined greatly influenced their permeation across silicone membranes. Furthermore, for a limited dataset, a significant correlation was identified between solute permeation across silicone membranes and that through human epidermis.

Conclusion. The key molecular properties that control solute permeation across silicone membranes have been identified. For the set of substituted phenols and other unrelated compounds examined here, a similar structure-permeation relationship has been derived for their transport through human epidermis, suggesting application of the results to the prediction of flux across biological barriers.

KEY WORDS: Silicone membrane permeability; phenols; hydrogen-bonding capacity; lipophilicity; skin transport.

INTRODUCTION

Transdermal drug delivery is an important area of pharmaceutical and toxicologic research. The skin acts as a highly efficient barrier preventing the ingress of xenobiotics and reducing water loss from the body. Notwithstanding this barrier property, the topical application of drugs is a promising route of administration whose potential advantages are well documented (1).

Understanding the physicochemical factors that control passive percutaneous absorption is a topic of current interest (2–4). Knowledge of these factors may allow one to predict the absorption characteristics of candidates for transdermal delivery. In this respect, many *in vivo* and *in vitro* experimental techniques have been used to elucidate the underlying diffusion mechanisms (5). However, the ultimate outcome of any model system is obviously its ability to yield observations in agreement with the more complex process it is meant to mimic. For percutaneous penetration, this means *in vivo* experiments in humans, which are often ethically unacceptable (e.g., during early-stage drug development), expensive, and time-consuming. Among the various models used to mimic *in vivo* experiments in humans, a wide variety of synthetic membranes may be identified (6).

The skin is a heterogeneous membrane, and it is recognized that the superficial stratum corneum most frequently controls percutaneous absorption, i.e., this layer represents the rate-determining step for diffusion (7). The lipoidal nature of the stratum corneum diffusion pathway suggests that artificial lipophilic membranes may provide useful *in vitro* models for permeation studies (8). Silicone membranes are of particular interest in this context (3,9,10).

The purpose of the present study was to characterize the mechanisms of permeation across silicone (polydimethylsiloxane) membranes by emphasizing the most distinctive structural parameters in a series of permeants. As previously described, the hydrogen-bonding capacity of compounds restricts their skin permeation (11). An initial set of substituted phenols was therefore chosen to evaluate how H-bonding influences permeation across such membranes, since in such compounds simple substitutions produce significant variations in H-bonding properties with only little change in other molecular parameters such as size and shape. In addition to these phenols, a small additional set of four drugs was also examined.

Experimental and computational parameters were used to quantify the H-bonding capacity. The experimental parameter was the difference between solute partition coefficients measured in two solvent systems ($\Delta\log P_{oct\text{-}dce}$; 12). The computational parameter was calculated by the molecular hydrogen-bonding potentials (MHBPs), which was recently developed in our laboratory (13). Permeation experiments were performed in a simple diffusion cell, and a mathematical model of pseudosteady-state diffusion was developed to determine the permeability coefficients.

MATHEMATICAL MODEL

The most commonly used method to analyze *in vitro* permeation data obtained by an infinite dose technique is the lag time method of the steady-state results (14). Whereas this approach is readily applicable, it is often difficult to determine when steady state is achieved, a serious shortcoming because a misleading interpretation at this stage can lead to large errors in permeation values (15). Furthermore, for this analysis to apply, concentrations in the receptor solution must be kept constant (usually at nearly zero) throughout the experiment. The pseudosteady-state method described here bypasses such a problem. Taking into account drug concentration buildup in the receiving chamber, the mathematical model removes the experimental constraint of maintaining sink conditions.

The experimental permeation method (Fig. 1) involved

[1] Institut de Chimie Thérapeutique, BEP, Université de Lausanne, CH-1015, Lausanne, Switzerland.
[2] Department of Chemical Engineering and Petroleum Refining, Colorado School of Mines, Golden, Colorado 80401.
[3] Centre Interuniversitaire de Recherche et d'Enseignement, Universities of Geneva and Lyon, ("Pharmapeptides"), F-74166 Archamps, France; University of Geneva, Faculty of Sciences, CH-1211 Geneva 4, Switzerland.
[4] To whom correspondence should be addressed. (e-mail: Bernard.Testa@ict.unil.ch)

0724-8741/02/1100-1622/0 © 2002 Plenum Publishing Corporation

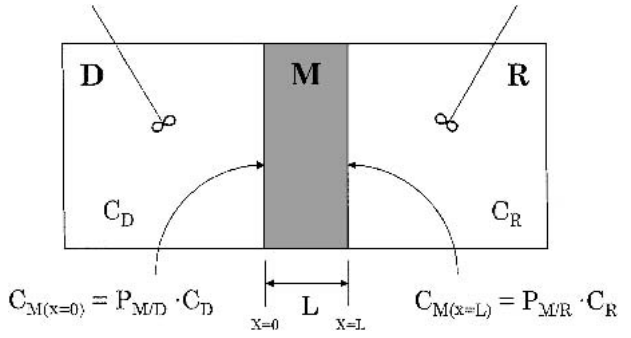

Fig. 1. Schematic diagram of the *in vitro* permeation experiment. M = membrane, D = donor chamber, R = receptor chamber.

placing a dilute solution of the test compound in the donor chamber (D) and monitoring the accumulation of that compound in the initially solute-free solution of the receiving chamber (R). A membrane of thickness L and area A separated the two well-stirred compartments (of volumes V_D and V_R, respectively) containing the same solvent. Assuming a one-directional flux, the solute diffused from the donor chamber (C_D), shown on the left-hand side of the membrane, into the less concentrated solution (C_R), shown on the right. This *in vitro* permeation system is described mathematically with a pseudosteady-state model as outlined in the Appendix (16) with the result:

$$\ln\left(\frac{C_D - C_R}{C_D^0}\right) = -\gamma \cdot t \tag{1}$$

in which

$$\gamma = \frac{A \cdot K_p}{V_D \cdot V_R} \cdot (V_D + V_R) \tag{2}$$

and K_p, the permeability coefficient, is defined as:

$$K_p = \frac{D_M \cdot P}{L} \tag{3}$$

where D_M is the diffusion coefficient in the membrane and P is the partition coefficient of the solute between the membrane and solvent. Plotting the negative natural logarithm of the concentration ratio against time, a straight line with a slope equal to γ is observed from which Kp can be determined as

$$K_p = \frac{\gamma \cdot V_D}{2 \cdot A} \tag{4}$$

in which it was assumed that $V_D = V_R$.

MATERIALS AND METHODS

Materials

2,6-Difluorophenol, 2,6-dichlorophenol, 2,6-dibromophenol, 2,5-dinitrophenol, and orphenadrine were purchased from Aldrich (Buchs, Switzerland). Phenol, 2-bromophenol, 4-bromophenol, 2-nitrophenol, 3-nitrophenol, 4-nitrophenol, 2,4-dinitrophenol, and nitrobenzene were obtained from Fluka (Buchs, Switzerland). Lidocaine and (S)-nicotine were provided by Sigma (Buchs, Switzerland) and diazepam by Lipomed (Arlesheim, Switzerland). The Silatos™ silicone sheeting (150 × 200 × 0.12 mm, d = 1.33 g/cm^3), a medical-grade dimethylsiloxane polymer, was purchased from Atos Medical (Hörby, Sweden). Analytical grade 1,2-dichloroethane (DCE) and *n*-octanol were obtained from Fluka (Buchs, Switzerland). All other reagents were of analytical grade and were used as received. Distilled water was used throughout.

pK_a Measurements

The protonation constants were determined by potentiometric titration using the GLpK_a apparatus (Sirius Analytical Instruments Ltd, Forrest Row, East Sussex, UK) as previously described (17). The low aqueous solubility of compounds **3, 4, 5, 6,** and **13** (Table I) required pK_a measurements in the presence of methanol as co-solvent. For acidic compounds, at least five separate 20-mL semi-aqueous solutions of ca. 1 mM, in 20–40% (w/w) methanol, were initially alkalinized to an appropriately high pH with standardized KOH. The solutions were then titrated with HCl 0.5 M to low pH (minimum 2.0). The same procedure was applied for basic compounds but the analysis ran from low to high pH (maximum 12.0) with standardized KOH. The titrations were conducted under an inert gas atmosphere (Ar) at 25.0 ± 0.1°C. The initial estimates of p_sK_a values (the apparent ionization constants in the H_2O/co-solvent mixture) were obtained from Bjerrum plots. These values were refined by a weighted non-linear least-squares procedure. The refined values were then extrapolated to zero percent of co-solvent by the Yasuda-Shedlovsky procedure (18).

Partition Coefficients Measurements

The partition coefficients in octanol/H_2O and DCE/H_2O were determined by the pH-metric method with the GLpK_a apparatus. The principle of the pH-metric method for pK_a and log P measurements has been explained in detail elsewhere (17,18). At least three separate titrations of compounds **1–15** (ca. 1 mM) were performed in the pH range 1.8 to 12.2 using various volumes of octanol or DCE (volume ratios of organic solvent/H_2O ranging from 0.3 to 0.8). All experiments were performed under Ar at 25.0 ± 0.1°C.

Assessment of Hydrogen-Bonding Capacity

$\Delta\log P_{oct\text{-}alk}$ has been shown to express essentially the capacity of solutes to donate hydrogen bonds (19). However, the determination of partition coefficients in alkane/water systems is often difficult because of the low solubility of many compounds. The DCE/water system appears to be a promising alternative by which to overcome these experimental constraints (12). Hence, the H-bond donor acidity of each drug was assessed by the difference ($\log P_{oct} - \log P_{dce}$).

In addition to experimental approaches to quantify a molecule's capacity to form hydrogen bonds, a computational tool—molecular hydrogen-bonding potentials (MHBPs)—has been recently described (13), composed of a H-bonding donor potential ($MHBP_{do}$) and a H-bonding acceptor potential ($MHBP_{ac}$), which are calculated in a stepwise procedure. First, a H-bonding fragmental system containing literature donor (α) and acceptor (β) values (20,21) was developed, as well as geometric functions relating the variations in potential with distance and angle. The fragmental system and the geo-

Table I. Experimental and Computational Physicochemic Parameters for the Compounds Studied

		Permeation		Physicochemic properties								
	Name	K_p[a] [cm/h]	log K_p	pK_a[b]	MW [g/mol]	log P_{oct}[c]	log P_{dce}[d]	Δlog P[e]	$MHBP_{ac}$[f]	$MHBP_{do}$[f]	Σf_{ac}[g]	Σf_{do}[g]
1	Phenol	0.129	–0.889	9.99	94.11	1.49	0.26	1.23	37.7	74.4	0.30	0.60
2	2,6-Difluorophenol	0.333	–0.478	7.09	130.10	2.05	0.93	1.12	38.8	71.6	0.31	0.60
3	2,6-Dichlorophenol	0.912	–0.040	6.91	163.0	2.75	2.12	0.63	39.3	40.3	0.31	0.36
4	2,6-Dibromophenol	1.521	0.182	6.53	251.92	3.36	2.94	0.41	39.7	40.3	0.31	0.36
5	2-Bromophenol	0.701	–0.154	8.32	173.02	2.35	1.78	0.57	38.7	45.3	0.31	0.36
6	4-Bromophenol	0.360	–0.444	9.13	173.02	2.59	1.51	1.08	24.8	83.7	0.20	0.67
7	2-Nitrophenol	1.233	0.091	6.92	139.11	1.79	2.81	–1.02	44.9	6.4	0.37	0.05
8	4-Nitrophenol	0.030	–1.527	6.90	139.11	1.91	0.72	1.19	28.9	101.1	0.26	0.82
9	3-Nitrophenol	0.045	–1.347	8.10	139.11	2.00	0.92	1.08	25.4	97.3	0.23	0.79
10	2,4-Dinitrophenol	0.300	–0.523	3.96	184.11	1.52	2.46	–0.94	56.5	6.1	0.49	0.05
11	2,5-Dinitrophenol	0.505	–0.297	4.97	184.11	1.75	2.49	–0.74	56.2	6.1	0.49	0.05
12	Nitrobenzene	2.009	0.303	—	123.11	1.85	3.13[h]	–1.28	27.5	0.0	0.28	0.00
13	Diazepam	0.450	–0.347	3.45	284.75	2.92	3.10	–0.18	70.9	0.0	0.71	0.00
14	Lidocaine	0.322	–0.493	7.94	234.40	2.33	3.16	–0.83	166.7	64.7	1.40	0.50
15	Nicotine	0.184	–0.735	8.08/3.21	162.24	1.23	1.21	0.02	131.8	0.0	1.25	0.00
16	Orphenadrine	22.289	1.348	9.10	269.39	3.84	4.52	–0.68	132.3	0.0	1.18	0.00

[a] Calculated permeation coefficient using the non-steady-state diffusion model and adjustment for ionization (see Eq. 5); n = 3; SD < 0.02.
[b] Determinated by potentiometry; n = 3; SD < 0.1.
[c] Logarithm of n-octanol/water partition coefficient determined by potentiometry; n = 3; SD < 0.02.
[d] Logarithm of 1,2-dichloroethane/water partition coefficient determined by potentiometry; n = 3; SD < 0.02.
[e] Difference between the log P_{oct} and log P_{dce} of a solute.
[f] MHBP calculated on the molecular surface for an acceptor (ac) or a donor (do) solute.
[g] Sum of the fragmental values of polar atoms (ac) or polar hydrogen atoms (do) in a solute.
[h] Measured by centrifugal partition chromatography, with pH 4.6 buffer as the stationary phase (12).

metric functions were then combined to generate the H-bonding potentials. These are calculated at each point of the molecular surface and the sums of the donor and acceptor potentials are the two parameters which characterize the molecular H-bonding capacity (∑MHBP).

Permeation Experiments

A wide variety of diffusion cell systems have been developed for use with rate-limiting membranes, but many show relatively poor mixing hydrodynamics and lack the possibility of automation (22). In this study, all *in vitro* experiments were performed with a specially designed diffusion cell consisting of two half compartments of 9 mL volume and an effective diffusion area of 2.0 cm^2. Silicone membranes were cut into round pieces of 24 mm in diameter and clamped between the two glass chambers using a Teflon joint. The membranes were immersed in distilled water for 1 h before use. The donor chamber was filled with a dilute drug solution (ca. 1 mM) and buffered to pH 4.0 (50 mM citrate-phosphate salts) for phenols or pH 7.4 (50 mM phosphate salts) for basic compounds. All buffers contained 5% EtOH (23,24) although the presence of the solvent was necessary only for the less soluble compounds. Both compartments were stirred with teflon-coated magnetic bars at 150 rpm; two other stirrers, connected to a motor, were positioned below the cell system to produce synchronous stirring in both cells. This entire device was fastened in a plexiglas cage and temperature controlled by immersion in a water bath at 37°C. Finally, the solution in each compartment was separately circulated through a flow-through cell (Hellma, type 176.700-QS, Müllheim, Germany) mounted in a spectrophotometer (Perkin Elmer, Lambda 11, Ueberlingen, Germany) using Teflon tubing (1/30 inches internal diameter, Zeus Industrial Products, Raritan, NJ, USA). A peristaltic pump set at 9 mL/min (Ismatec, Reglo FMI 005, Glattbrugg, Switzerland) allowed on-line measurements in the chambers and data collection by a computer connected to the spectrophotometer.

It must be noted, however, that the low permeation of relatively hydrophilic solutes (log P_{oct} < 1) precluded the accurate determination of their K_p.

Adjustment for Ionization

Permeability coefficients were measured for chemicals with different ionization behavior. Some of the analyzed compounds were essentially neutral at the experimental pH, whereas others were partly or mostly ionized. As a first approximation, penetration can be attributed to the neutral species alone, particularly when the percent unionized is greater than 10%. Consequently, the permeation coefficients of unionized species were calculated by dividing the observed permeability coefficient, based on the total concentration, by the unionized fraction (f_{ui}). For compounds with a single acid-base reaction, this parameter is correlated to the dissociation constant (pK_a) and the pH of the donor chamber by the following equation:

$$f_{ui} = \frac{1}{(1 + 10^{g})} \quad (5)$$

where the exponent $g = (\text{pH} - pK_a)$ for acids and $(pK_a - \text{pH})$ for bases.

RESULTS AND DISCUSSION

The experimental and computational physicochemic parameters for the two sets of compounds are summarized in Table I. All experiments were performed at a fixed pH value of 4.0 or 7.4 for the initial or additional set, respectively, and the calculated permeation coefficients were adjusted for ionization according to Eq. 5.

Permeability of Phenolic Compounds across Silicone Membranes

Effect of Lipophilicity

The actual partition coefficient between a membrane and the bathing solution is a key determinant of permeability. In this study, the amphiprotic *n*-octanol and the inert (DCE) were chosen as surrogate models. As revealed by Fig. 2(A and B) log P_{dce} describes solute permeation across silicone membranes better than log P_{oct}. The reason may be that the polydimethylsiloxane membrane, like DCE but unlike octanol, has little ability to form hydrogen bonds (see below). Moreover, although there is a general trend of increasing permeability with lipophilicity in DCE as depicted in Fig. 2B, two distinct groups of compound are apparent in the graph. The first represents the halophenols, the second the nitroderivates. As is readily appreciated, lipophilicity is strongly influenced by the nature of the substituents and by their position around the aromatic ring.

Effect of Hydrogen-Bonding Capacity

This property has often been used in structure-permeation relationships and is related to skin permeation (11,25). Different experimental approaches can be used to assess H-bonding capacity; e.g., the solvatochromic parameters α (H-bond donor acidity) and β (H-bond acceptor basicity) (26–28). The $\Delta\log P_{oct\text{-}dce}$ ($\log P_{oct} - \log P_{dce}$) parameter expresses mainly the hydrogen-bond donor acidity of a solute (12). Indeed, log P_{oct} contains no contribution from the solute H-bond donor capacity, unlike log P_{dce} of which it is a major component.

The separation between the two groups of compounds seen in Fig. 2B (the halophenols and the nitro-derivates) is clearer in Fig. 2C. For the halophenols, the $\Delta\log P_{oct\text{-}dce}$ parameter decreases when the substituent is located close to the hydroxy group; compare, for example, 2-bromophenol (**5**) and 4-bromophenol (**6**). The presence of a halo-atom in the ortho- rather than para-position weakens the H-bond donor acidity of the –OH moiety due to proximity effects, and facilitates permeability across the polymer membrane (see later Table I).

For the nitrophenols, the influence of the substitution pattern on membrane permeability can be summarized as follows. First, the presence of a single phenolic group produces a positive Δlog *P* value relative to non-H-bond forming solutes. The lower log P_{dce} relative to log P_{oct} is consistent with the fact that DCE does not form H-bonds with solutes. The presence of nitro substituents in the para- or metaposition means that the phenolic group predominates over the nitro group in terms of $\Delta\log P_{oct\text{-}dce}$ value. The hydrogen-bond donor acidity of para-nitrophenol is slightly reinforced compared to meta-nitrophenol due to an inductive effect, thereby decreasing its permeability. Finally, the $\Delta\log P_{oct\text{-}dce}$ values of ortho-substituted phenols are significantly reduced due to their high log P_{dce} values, indicating that this H-bond donor capacity is not expressed in the DCE/water system. A strong

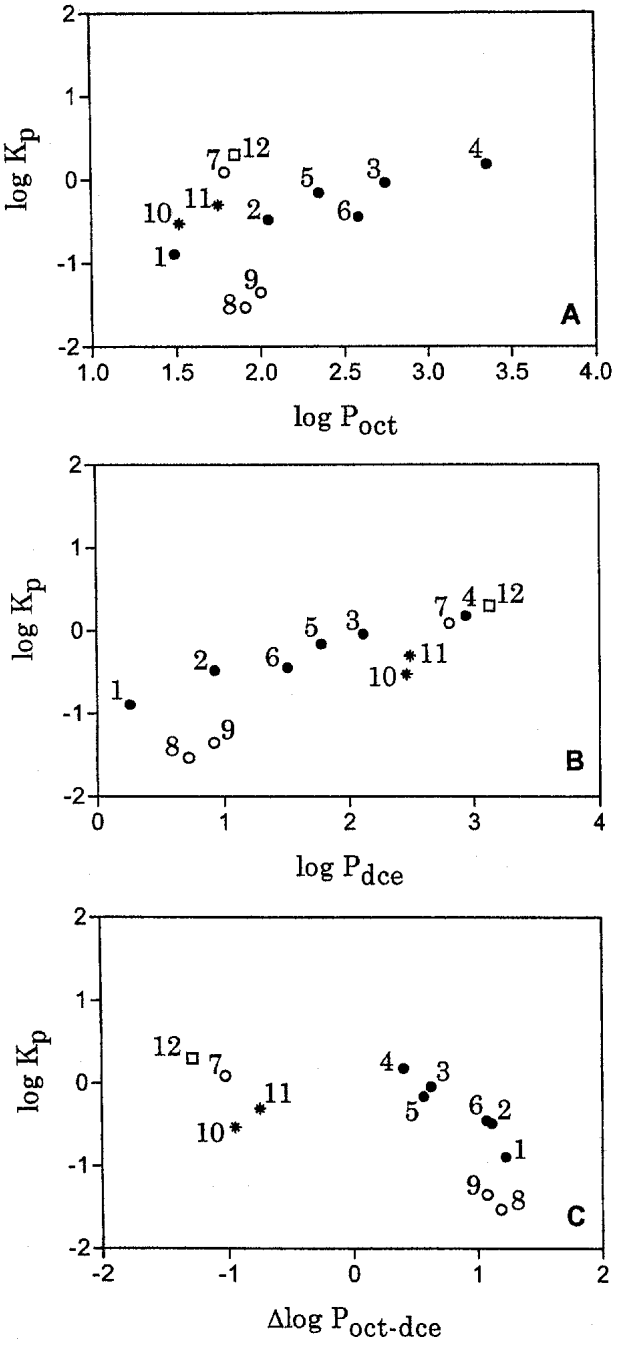

Fig. 2. Permeability of the initial set of compounds across silicone membranes as a function of lipophilicity measured in terms of n-octanol/water partitioning (A), 1,2-dichloroethane/water distribution (B), and by the difference between these two solvent systems (C). ● halophenols, dihalophenols and phenol, ○ nitrophenols, ✳ dinitrophenols, □ nitrobenzene. Compound numbering follows that in Table I.

intramolecular hydrogen bond between the nitro group and the phenolic function accounts for this behavior.

The strong stabilization of this intramolecular H-bond in nonpolar solvents (29) renders these compounds much more lipophilic than other nitrophenols in the DCE/water system. In the octanol/water system, the large amount of water in the organic phase offers additional possibilities for the formation of intermolecular H-bonds, which compete with intramolecular H-bonds and affect the lipophilicity ranking of these compounds (Table I).

In addition to experimental approaches to quantify a molecule's capacity to form hydrogen bonds, a computational tool—MHBPS—has been developed (13). Examples of such calculated potentials are illustrated in Fig. 3 for ortho and para-nitrophenol. The H-bonding acceptor potential on the molecular surface of 4-nitrophenol (Fig. 3A) and 2-nitrophenol (Fig. 3C) are similar, in stark contrast to their H-bonding donor potential (Fig. 3B) and (Fig. 3D), respectively. Indeed, the presence of an intramolecular interaction greatly decreases or abolishes the H-bonding donor capacity of a solute. As depicted in Fig. 3B and the corresponding parameters of the linear regression (n = 12, r^2 = 0.60, q^2 = 0.40), a major determinant of diffusion across silicone membranes is clearly the H-bond donor acidity but not the H-bond acceptor basicity (Fig. 4A). This observation agrees with the permeation results from human skin experiments (3). Moreover, Fig. 4B illustrates the influence of an ortho-nitro group on the MHBPs. As can be seen, the dinitrophenols (**10, 11**) deviate from the linear relationships between H-bonding capacity and permeation through silicone membranes, suggesting that other factors beside H-bonding influence permeation. Several studies based on silicone membrane permeation support this observation.

The results obtained support, complement and extend the extensive body of work by Matheson *et al.* (30,31) on the transport of a considerable number of aromatic and heterocyclic compounds across silicone membranes. These earlier publications highlighted the use of physicochemic properties, such as hydrophobic fragmental constants, molar refractivity (chosen as a volume parameter), Hammett's constants taking into account substituent electronic effects, mole fraction solubility in isopropyl alcohol and melting point, to develop predictive models. It was also shown using comparative molecular field analysis and atomic charge calculations that other parameters, including molecular weight and intramolecular hydrogen bonding potential, for example, contributed to the determination of permeation flux (32–34).

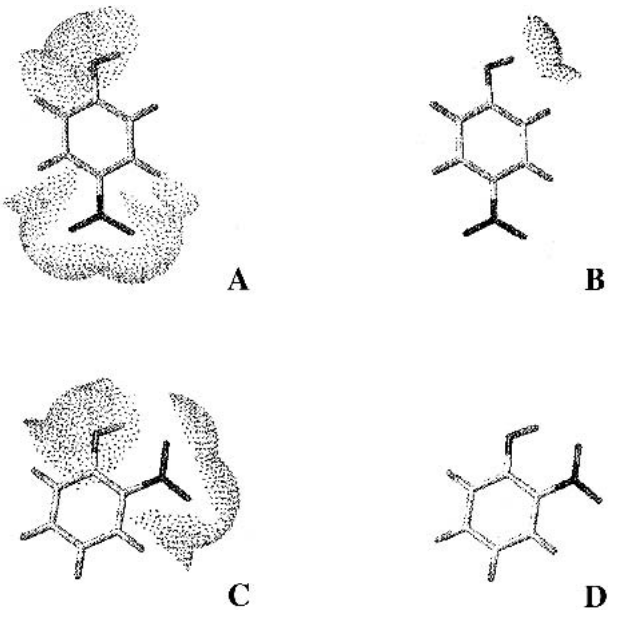

Fig. 3. Calculated molecular H-bonding acceptor and H-bonding donor potentials of 4-nitrophenol (A and B, respectively) and 2-nitrophenol (C and D, respectively).

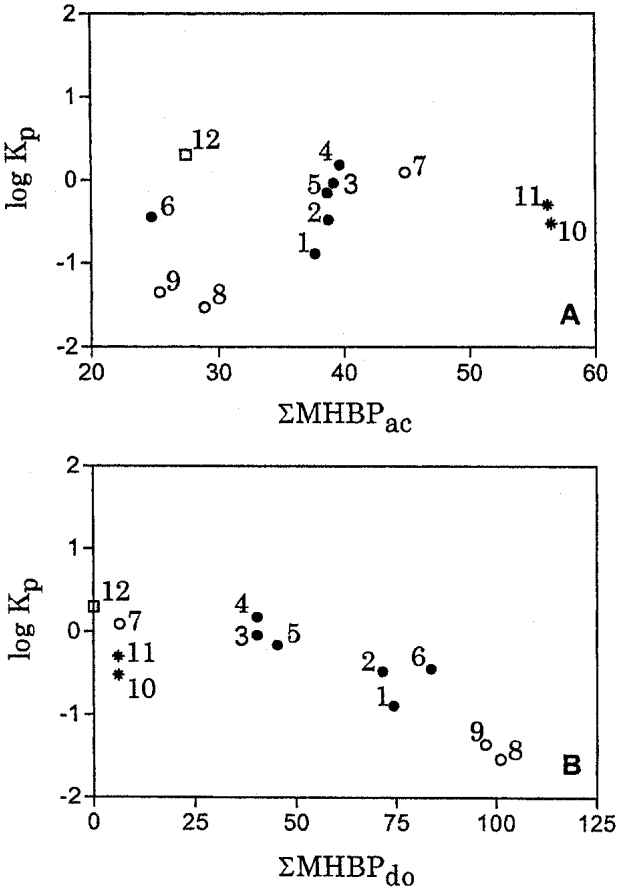

Fig. 4. Permeability of the initial set of compounds across silicone membranes as a function of their molecular H-bonding acceptor (A) and donor (B) potential. ● halophenols, dihalophenols and phenol, ○ nitrophenols, ❋ di-nitrophenols, □ nitrobenzene.

Permeability of Selected Drugs across Silicone Membranes

A set of four additional drugs was investigated to assess the generality of the previous observations. The influence of physicochemical and structural variability was therefore analyzed over an extended range of lipophilicity and molecular weight compared to the initial set.

As seen in Fig. 5, log P_{dce} is a significant parameter for the prediction of solute permeability across silicone membranes. As mentioned above, the major contributions to log P_{dce} are hydrophobicity and H-bond donor acidity (12). Equation 6 illustrates the linear relationship between permeability coefficient and partition coefficient in DCE/water; that is, a single parameter allows a fair prediction of permeability:

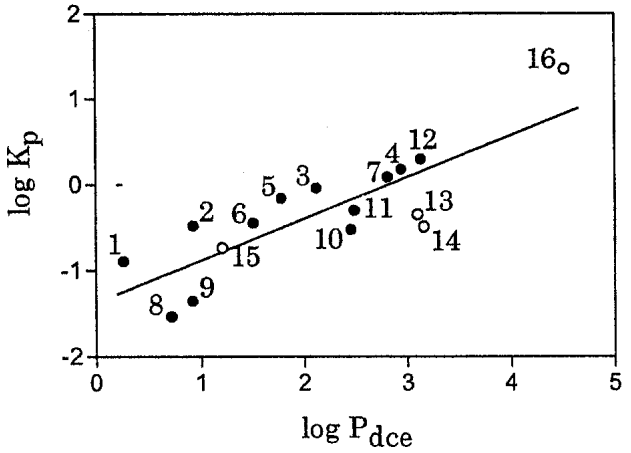

Fig. 5. Permeability of the initial set (●) and additional set of compounds (○) through silicone membranes as a function of lipophilicity in the 1,2-dichloroethane/water system (Eq. 6).

$$\log K_p = 0.49\ (\pm 0.26) \cdot \log P_{dce} - 1.36\ (\pm 0.55)$$
$$n = 16;\ r^2 = 0.70;\ q^2 = 0.56;\ s = 0.38;\ F = 32 \qquad (6)$$

In this and the following equations, 95% confidence limits are given in parentheses; n is the number of compounds, r^2 the squared correlation coefficient, q^2 the cross-validated correlation coefficient, s the standard deviation, and F the Fischer's test.

The hydrogen-bonding donor acidity is a relevant parameter which greatly influences permeation across polydimethylsiloxane membranes. Adding the four drugs to the linear regression between log K_p and $MHBP_{do}$ yields a poorer correlation (n = 16, r^2 = 0.42, q^2 = 0.22) because diazepam, nicotine, and orphenadrine have no H-bond donor capacity. However, a better relationship is recovered by adding log P_{oct} in the multilinear Eq. 7:

$$\log K_p = 0.56\ (\pm 0.37) \cdot \log P_{oct} - 0.0108\ (\pm 0.0064) \cdot \sum MHBP_{do} - 1.16\ (\pm 0.72)$$
$$n = 16;\ r^2 = 0.77;\ q^2 = 0.61;\ s = 0.35;\ F = 21 \qquad (7)$$

Statistically, Eq. 7 is comparable with Eq. 6. This shows that predictions of silicone membrane permeation can be based on the single log P_{dce} parameter (Eq. 6), which expresses the same intermolecular forces as the combined log P_{oct} and a H-bond donor parameter (e.g., $\sum MHBP_{do}$ in Eq. 7, or $\Delta \log P$; 12,28).

Comparison with Human Skin Permeation

As silicone membranes are artificial barriers used to model skin lipids (3,6), the membrane permeability coefficients ($K_{p(sil)}$) of seven compounds were compared to their corresponding *in vitro* values across human epidermis ($K_{p(epid)}$; Fig. 6) The correlation was good (Eq. 8):

$$\log K_{p(sil)} = 1.15\ (\pm 0.36) \cdot \log K_{p(epid)} + 1.29\ (\pm 0.58)$$
$$n = 7;\ r^2 = 0.90;\ q^2 = 0.83;\ s = 0.19;\ F = 46 \qquad (8)$$

As indicated by the positive intercept in Eq. 8, the permeability through silicone membrane is about 10 times higher than that through excised human skin (Table II). The relationship indicates that silicone membranes may be a useful trend-predictive model for skin permeation.

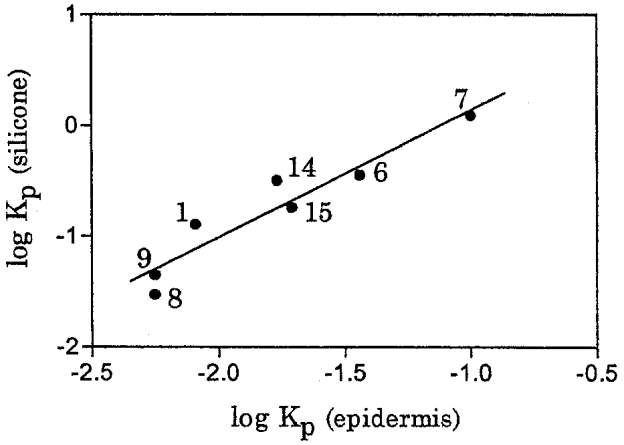

Fig. 6. Correlation of solute permeabilities through human epidermis (36,37) and silicone membranes. See Table II for data and Eq. 8.

CONCLUSION

This study demonstrates that the permeation of xenobiotics across polydimethylsiloxane membranes is controlled primarily by their H-bond donor capacity, in turn strongly influenced by intramolecular interactions. Lipophilicity also plays a role. Thus, a single H-bond donor parameter is shown to correlate with silicone membrane permeability for a congeneric set of phenols, whereas a lipophilicity term must be added when heterogeneous drugs are included in the regression (Eq. 7). Interestingly, the permeation of the extended set is also well described by lipophilicity in the dichloroethane/water system (log P_{dce}, Eq. 6), which encodes a strong contribution from H-bond donor capacity (12), in contrast to log P_{oct} which does not.

ACKNOWLEDGMENTS

Financial support was provided by the Fonds national suisse de la recherche scientifique, and by the Programme commun de recherche en génie biomédicale (Universities of Geneva and Lausanne, and the Ecole polytechnique fédérale, Lausanne).

APPENDIX

Development of the Mathematical Model

The key assumptions are the following: (1) depletion of the donor chamber; (2) accumulation in the receiving cham-

Table II. Experimental Permeability Coefficients of Selected Compounds through Silicone Membranes and across Human Epidermis

		Silicone membrane		Human epidermis[a]	
	Chemical	K_p [cm/h]	log K_p	K_p [cm/h]	log K_p
1	Phenol	0.129	–0.889	0.008	–2.090
6	4-Bromophenol	0.360	–0.444	0.036	–1.440
7	2-Nitrophenol	1.233	0.091	0.100	–1.000
8	4-Nitrophenol	0.030	–1.527	0.006	–2.250
9	3-Nitrophenol	0.045	–1.347	0.006	–2.250
14	Lidocaine	0.322	–0.493	0.017	–1.770[b]
15	Nicotine	0.184	–0.735	0.019	–1.710

[a] Data from Flynn *et al.* (36).
[b] Data from Johnson *et al.* (37).

ber; (3) instantaneous equilibrium at the skin-solution interfaces; (4) a homogeneous membrane as the barrier to diffusion (5) a constant diffusion coefficient; (6) no binding or metabolism within the membrane; (7) no solvent diffusion.

To determine the solute concentration profile and the flux across the membrane, it is necessary to write three unsteady-state solute mass balances:

membrane M: $$\frac{\partial C_M}{\partial t} = D_M \cdot \frac{\partial^2 C_M}{\partial x^2} \quad \text{(A1)}$$

donor chamber D: $$\frac{V_D}{A} \cdot \frac{dC_D}{dt} = D_M \cdot \left.\frac{\partial C_M}{\partial x}\right|_{x=0} \quad \text{(A2)}$$

receptor chamber R: $$\frac{V_R}{A} \cdot \frac{dC_R}{dt} = -D_M \cdot \left.\frac{\partial C_M}{\partial x}\right|_{x=L} \quad \text{(A3)}$$

where C is the concentration of the permeant expressed in g/cm^3, V is the volume in cm^3 of each chamber, D_M is the diffusion coefficient in the membrane in cm^2/s, A is the area of the membrane in cm^2, and x is the depth in membrane M.

These differential equations are subject to the following specific conditions:

at $t = 0$, $$C_D = C_D^0,\ C_R = 0,\ C_M = 0 \quad \text{(A4)}$$

at $x = 0$, $$C_M = P_{M/D} \cdot C_D \quad \text{(A5)}$$

at $x = L$, $$C_M = P_{M/R} \cdot C_R \quad \text{(A6)}$$

If the two compartments contain the same solvent conditions, the following simplification is allowed: $P_{M/D} = P_{M/R} = P$. Described as the partition coefficient of the solute between the membrane and solvent, this latter parameter is assumed not to vary with solute concentration.

Moreover, if $P \cdot L \cdot A << V$, the amount of solute in the membrane will be always negligible compared with the amount of solute in the two compartments. As a result, the variation in concentration in the donor and receptor solutions will be slow compared to the diffusion rate across the membrane. In other words, the concentration profile across the membrane will always be close to its steady-state value, even though the compartment concentrations are time-dependent. This suggests that a pseudosteady-state solution strategy is appropriate.

Assuming pseudosteady state, where the rate of change of concentration, $\partial C_M/\partial t$, will be zero, Eq. A1 is first integrated twice and combined with Eqs. A5 and A6, to obtain the following expression for the concentration profile

$$C_M = P \cdot C_D - \frac{P}{L} \cdot x \cdot (C_D - C_R) \quad \text{(A7)}$$

Eq. A7 is differentiated and evaluated at $x = 0$ and $x = L$ to obtain:

$$\left.\frac{\partial C_M}{\partial x}\right|_{x=0} = \left.\frac{\partial C_M}{\partial x}\right|_{x=L} = -\frac{P}{L}(C_D - C_R) \quad \text{(A8)}$$

It has been shown that it is experimentally more robust to analyze the data as the difference $[C_D(t) - C_R(t)]$ rather than either $C_D(t)$ or $C_R(t)$ individually (14). Subtracting Eq. A3 from Eq. A2 and substituting for Eq. A8 yields the following:

$$\frac{d}{dt}(C_D - C_R) = -\gamma \cdot (C_D - C_R) \quad \text{(A9)}$$

in which γ is defined by Eq. 2.

Eq. A9 is solved subject to the initial condition Eq. A4 to give:

$$\ln\left(\frac{C_D - C_R}{C_D^0}\right) = -\gamma \cdot t \quad \text{(A10)}$$

This pseudosteady-state analysis holds as long as $P \cdot L \cdot A/V_D < \sim 0.1$, assuming that $V_D = V_R$ (35).

REFERENCES

1. J. Hadgraft and R. H. Guy. *Transdermal Drug Delivery-Development Issues and Research Initiatives.* Marcel Dekker, New York, 1989.
2. R. O. Potts and R. H. Guy. Predicting skin permeability. *Pharm. Res.* **9**:663–669 (1992).
3. M. T. D. Cronin, J. C. Dearden, G. P. Moss, and G. Murray-Dickson. Investigation of the mechanism of flux across human skin *in vitro* by quantitative structure–permeability relationships. *Eur. J. Pharm. Sci.* **7**:325–330 (1999).
4. L. A. Kirchner, R. P. Moody, E. Doyle, R. Bose, J. Jeffery, and I. Chu. The prediction of skin permeability by using physicochemical data. *ATLA* **25**:359–370 (1997).
5. N. Sekkat and R. H. Guy. Biological models to study skin permeation. In: B. Testa, H. van de Waterbeemd, G. Folkers, and R. H. Guy (eds.), *Pharmacokinetic Optimization in Drug Research: Biological, Physicochemical and Computational Strategies.* Wiley-VCH, Zurich, 2001 pp. 155–172.
6. J. Houk and R. H. Guy. Membrane models for skin penetration studies. *Chem. Rev.* **88**:455–471 (1988).
7. J. Hadgraft and W. J. Pugh. The selection and design of topical and transdermal agents: A review. *J. Invest. Dermatol.* **3**:131–135 (1998).
8. G. Ridout, J. Houk, R. H. Guy, G. C. Santus, J. Hadgraft, and L. L. Hall. An evaluation of structure-penetration relationships in percutaneous absorption. *Farmaco* **47**:869–892 (1992).
9. E. R. Garrett and P. B. Chemburkar. Evaluation, control, and prediction of drug diffusion through polymeric membranes. *J. Pharm. Sci.* **57**:944–948 (1968).
10. J. du Plessis, W. J. Pugh, A. Judefeind, and J. Hadgraft. The effect of hydrogen bonding on diffusion across model membranes: consideration of the number of H-bonding groups. *Eur. J. Pharm. Sci.* **13**:135–141 (2001).
11. R. O. Potts and R. H. Guy. A predictive algorithm for skin permeability: The effects of molecular size and hydrogen bond activity. *Pharm. Res.* **12**:1628–1633 (1995).
12. G. Steyaert, G. Lisa, P. Gaillard, G. Boss, F. Reymond, H. H. Girault, P. A. Carrupt, and B. Testa. Intermolecular forces expressed in 1,2-dichloroethane/water partition coefficient: A solvatochromic analysis. *J. Chem. Soc. Faraday Trans.* **93**:401–406 (1997).
13. S. Rey, G. Caron, G. Ermondi, P. Gaillard, A. Pagliara, P. A. Carrupt, and B. Testa. Development of molecular hydrogen bonding potentials (MHBPs) and their application to structure permeation relations. *J. Mol. Graphics Model.* **19**:521–535 (2001).
14. B. W. Barry. *Dermatological Formulations.* Dekker, New York, 1983.
15. J. C. Shah. Analysis of permeation data: evaluation of the lag time method. *Int. J. Pharm.* **90**:161–169 (1993).
16. E. L. Cussler. *Diffusion: Mass Transfer in Fluid Systems, 2nd Ed.* Cambridge University Press, New York, 1997.
17. A. Avdeef. pH-Metric log P. Part 1. Difference plots for determining ion-pair octanol-water partition coefficients of multiprotic substances. *Quant. Struct.-Act. Relat.* **11**:510–517 (1992).
18. A. Avdeef, J. E. A. Comer, and S. J. Thomson. pH-Metric log P. 3. Glass electrode calibration in methanol-water, applied to pK_a determination of water-insoluble substances. *Anal. Chem.* **65**:42–49 (1993).
19. N. El Tayar, R. S. Tsai, B. Testa, P. A. Carrupt, and A. Leo.

Partitioning of solutes in different solvent systems: the contribution of hydrogen-bonding capacity and polarity. *J. Pharm. Sci.* **80**:590–598 (1991).
20. M. H. Abraham. Scales of solute hydrogen-bonding: Their construction and application to physicochemical and biochemical processes. *Chem. Soc. Rev.* **22**:73–83 (1993).
21. M. H. Abraham. Hydrogen bonding. 31. Construction of a scale of solute effective or summation hydrogen-bond basicity. *J. Phys. Org. Chem.* **6**:660–684 (1993).
22. D. R. Friend. *In vitro* skin permeation techniques. *J. Control. Release* **18**:235–248 (1992).
23. E. R. Garrett and P. B. Chemburkar. Evaluation, control, and prediction of drug diffusion through polymeric membranes. II. *J. Pharm. Sci.* **57**:949–959 (1968).
24. R. E. Kasting. *Synthetic Polymeric Membranes. A structural perspective, 2nd Ed.* Wiley, New York, 1985.
25. M. H. Abraham, H. S. Chadha, and R. C. Mitchell. The factors that influence skin penetration of solutes. *J. Pharm. Pharmacol.* **47**:8–16 (1995).
26. R. W. Taft, J. L. M. Abboud, M. J. Kamlet, and M. H. Abraham. Linear solvation energy relations. *J. Sol. Chem.* **14**:153–186 (1985).
27. R. W. Taft, M. H. Abraham, R. M. Doherty, and M. J. Kamlet. The molecular properties governing solubilities of organic nonelectrolytes in water. *Nature* **313**:304–306 (1985).
28. N. El Tayar, R. S. Tsai, B. Testa, P. A. Carrupt, C. Hansch, and A. Leo. Percutaneous penetration of drugs: A quantitative structure-permeability relationship study. *J. Pharm. Sci.* **80**:744–749 (1991).
29. H. van de Waterbeemd. *Hydrophobicity of Organic Compounds.* CompuDrug International, Vienna, 1986.
30. M. W. Hu and L. E. Matheson. The development of predictive method for the estimation of flux through polydimethylsiloxane membranes. III. Application to a series of substituted pyridines. *Pharm. Res.* **10**:732–736 (1993).
31. L. E. Matheson and M. W. Hu. The development of a predictive method for the estimation of flux through polydimethylsiloxane membranes. IV. Application to a series of substituted quinolines. *Pharm. Res.* **10**:839–842 (1993).
32. Y. Chen, W-L. Yang, and L. E. Metheson. Prediction of flux through polydimethylsiloxane membranes using atomic charge calculations. *Int. J. Pharm.* **94**:81–88 (1993).
33. R. Liu and L. E. Matheson. Comparative molecular field analysis combined with physicochemical parameters for prediction of polydimethylsiloxane membrane flux in isopropanol. *Pharm. Res.* **11**:257–266 (1994).
34. Y. Chen, P. Vayumhasuwan, and L. E. Matheson. Prediction of flux through polydimethylsiloxane membranes using atomic charge calculations: Application to an extended data set. *Int. J. Pharm.* **137**:149–158 (1996).
35. R. Mills, L. A. Woolf, and R. O. Watts. Simplified procedures for diaphragm-cell diffusion studies. *AlChE J.* **14**:671–673 (1968).
36. G. L. Flynn. Physicochemical determinants of skin absorption. In T. R. Gerrity and C. J. Henry (eds.), *Principles of Route-to-Route Extrapolation for Risk Assessment.* Elsevier, Amsterdam, 1990 pp. 93–127.
37. J. E. Johnson, D. Blankstein, and R. Langer. Evaluation of solute permeation through the stratum corneum: lateral bilayer diffusion as the primary transport mechanism. *J. Pharm. Sci.* **86**:1162–1172 (1997).